Solvent and Structural Effects on Ultrafast Chelation Dynamics of Arene Chromium Tricarbonyl Sulfide Derivatives

*Tung T. To[#] and Edwin J. Heilweil**

Optical Technology Division, National Institute of Standards and Technology, Gaithersburg, Maryland 20899-8443

edwin.heilweil@nist.gov

Charles B. Duke III and Theodore J. Burkey

Department of Chemistry, Campus Box 526060, University of Memphis, Memphis, Tennessee 38152-6060

tburkey@memphis.edu

NIST Guest Researcher/Postdoctoral Associate

Abstract

The chelation dynamics of three new [Cr{η^6-$C_6H_5C(O)R$}$(CO)_3$] complexes **1** (R = $CH_2(SCH_3)$), **2** (R = $CH(SCH_3)_2$), and **3** (R = $C(SCH_3)_3$) have been investigated on the picosecond to millisecond timescales by UV-pump IR-probe transient absorption spectroscopy following photodissociation of CO in room temperature *n*-heptane, tetrahydrofuran (THF), and acetonitrile. In *n*-heptane, UV irradiation of **1**, **2**, or **3** dissociates CO to initially yield a Cr-S chelate and a transient Cr-heptane solvate in approximately 1:2, 1:2, and 2:1 ratios, respectively. The Cr-heptane solvate is unstable and converts to the Cr-S chelate within 30 ns in each case. Irradiation of **2** or **3** in THF yields both the Cr-S chelate and Cr-THF solvate in approximately 1:3 and 1:1 ratios, respectively. The Cr-THF solvate converts to the Cr-S chelate on the second or longer timescale. All three complexes appear to yield the Cr-$NCCH_3$ solvate exclusively within 50 ps following irradiation in acetonitrile. The solvent effect on chelation is in striking contrast to that previously reported for the analogous $RCpMn(CO)_3$ derivatives, **4**-**6**. While irradiation of the Cr and Mn series in heptane results in picosecond chelation and solvent coordination, only chelation is observed for the Mn series while only solvate is observed for the Cr series in acetonitrile.

Introduction

Reversible molecular photoswitches have potential applications as recordable media and reversible optical switches,[1] and new, bistable, photochromic organometallics were recently reported.[2] High quantum yields, rapid response rates, and low fatigue are desirable properties of molecular photoswitches. In an effort to learn how to control and optimize these properties during the linkage isomerization of organometallic chelates, we have investigated several model organometallic compounds capable of chelation following CO photodissociation. Previous studies indicate that the structure of the chelatable functional groups and reaction environment can greatly influence the quantum yield, reaction rate, and chelation pathways of organometallic complexes.[3] For example, unit quantum yields were reported for chelation following CO photodissociation of $[Mn\{\eta^5\text{-}C_5H_4R\}(CO)_3]$ where R = $C(O)CH_2SCH_3$ and R = $CH_2CO_2CH_3$.[3c] These were the first examples unit quantum yields for organometallic photosubstitution. For R = $C(O)CH_3$, where no chelate can form and only CO photosubstitution with free nucleophile is observed, the quantum yield is 0.82.

Interestingly, a unit quantum yield indicates there can be no CO recombination. If chelation competes with geminate CO recombination,[4] which can occur within 300 fs,[5] then the chelation must be ultrafast. UV pump/IR probe transient ps to μs infrared experiments of **4**, **5**, and **6** (Chart 1) show that UV irradiation of these complexes induces ultrafast CO loss to eventually yield the stable Mn-S chelate in which the pendant sulfide moiety is coordinated with the unsaturated manganese metal center.[3b,c] This chelation process can occur via two pathways: a direct subpicosecond chelation pathway and a slower (> ns) intermediate solvent coordination pathway (Scheme 1). It appears that the

fast chelation pathway depends on the close proximity of a sulfide group to the metal center; otherwise, the slower solvent coordination pathway occurs. Molecular structure calculations show that the sulfide group(s) in **4** and **5** spend at least half of the time away from the metal center, whereas there is always a sulfide group near the metal center in **6**.[3b,c] Thus, only **6** can eliminate solvent coordination upon UV irradiation in alkane solution. In contrast, all three manganese complexes follow a direct chelation pathway upon UV irradiation in acetonitrile.[3a] While acetonitrile can form a stable Mn-acetonitrile adduct,[2] solvent effects apparently position the sulfide group(s) in **4** and **5** near the metal center thus allowing the Mn-S chelate to form before the unsaturated metal encounters acetonitrile.

To understand how the metal center and the structure of the chelating ligand may affect chelation rates and pathways, we prepared three new derivatives of the Cr species, **1**, **2**, and **3**, bearing identical sulfide side chains as the analogous Mn species, **4**, **5**, and **6**, respectively (Chart 1). In this report, we describe the photoinduced dynamics of **1**, **2**, and **3** in three solvents, *n*-heptane, tetrahydrofuran (THF), and acetonitrile and compare them to our earlier studies of **4**, **5**, and **6**.

Experimental Section

A detailed description of the time-resolved UV-pump infrared probe (TRIR) apparatus used for this study was previously reported.[3] In a typical experiment with picosecond time resolution, a 289 nm UV pulse (ca. 120 fs pulse duration with 4 μJ to 6 μJ energy) was focused to approximately 100 μm diameter in a 2 mm pathlength flow cell with CaF_2 windows. For nanosecond to millisecond resolution, 355 nm harmonic pulses from a Q-

switched Nd:YAG laser (4 ns pulse duration, 30 µJ to 40 µJ energy), were electronically synchronized and timed to the femtosecond IR probe pulses. We averaged 2000 laser shots to obtain a single difference spectrum. Two to four of these spectra were averaged for each time delay presented. Analysis of averaged spectra (typically four) yielded an intensity uncertainty from the baseline of less than ± 0.005 optical density (OD) units (k = 1; type B analysis).

To prepare samples for the TRIR experiments, the Cr complexes (30 mg to 50 mg) were dissolved in 50 mL to 80 mL of solvent to produce millimolar concentrations (e.g. 1.2 x 10^{-3} mol/L from 30 mg of **1** in 80 mL of *n*-heptane) with optical density (OD) ~ 1 measured at the higher CO-stretching frequency (e.g. near 1990 cm^{-1} in heptane) of the two Cr-CO-stretching bands. All samples were studied at room temperature (ca. 293 K).

Preparation of 1, 2, and 3

Previously reported syntheses of **5** and **6**[3ab] and 2,2-bis(methylthio)-1-phenylethanone and 2,2,2-tris(methylthio)-1-phenylethanone[6] were modified to produce **1**, **2**, and **3**. Tris(methylthio)methane (2.9 mL, 22 mmol) in 40 mL THF (tetrahydrofuran) was added to BuLi (12.5, 25 mmol, 2 M in pentane) and stirred at 195 K for 2 h. Methyl benzoate chromium tricarbonyl (2.0 g, 7.3 mmol) in 10 mL THF was added, and the solution was allowed to warm to room temperature overnight. Upon quenching with water, extraction of the aqueous phase with ether, and evaporation of the organic phase, the product was eluted with hexane/ethyl acetate on silica gel, yielding 93 mg (6.4 %) of red powder **1**.[7] Similar procedures were used to produce 0.8 g (62 %) of red crystalline **2** from tris(methylthio)methane (1.0 mL, 7.2 mmol) in 5 mL THF and BuLi (4.0 mL, 8.0 mmol,

2 M in pentane) (stirred at 175 K), and methyl benzoate chromium tricarbonyl (1.0 g, 3.7 mmol) in 10 mL THF.[8] To prepare **3**, tris(methylthio)methane (0.7 mL, 5.0 mmol) in 10 mL THF and BuLi (2.3 mL, 4.5 mmol, 2 M in pentane) were stirred at 175 K for 2 h. Methyl benzoate chromium tricarbonyl (2.7 g, 10.0 mmol) in 25 mL THF was added.[9] After stirring at 175 K for 4 h the resulting solution was quenched with water, the aqueous phase was extracted with ether, and the organic phase was concentrated by evaporation overnight yielding 1.0 g (53 %) of red crystalline **3**.

Acetonitrile (anhydrous), tris(methylthio)methane, butyllithium (BuLi), methylbenzoate, THF (anhydrous), and tris(methyl)thiomethane were obtained from Sigma-Aldrich Chemicals; *n*-heptane (analytical grade) from the Mallinckrodt Chemicals, and $Cr(CO)_6$ from Strem Chemical and were used without further purification.[10] Methyl benzoate chromium tricarbonyl was synthesized from methylbenzoate and $Cr(CO)_6$ according to literature procedures.[11]

Results and Discussion

TRIR experiments performed in this work show that irradiation of **1**, **2**, or **3** in *n*-heptane solution at either 289 nm or 355 nm results in CO dissociation to initially form two photoproducts: the transient Cr-heptane solvate and stable Cr-S bound chelate. The Cr-heptane solvate eventually converts to the Cr-S chelate on the nanosecond timescale. Examining the difference TRIR spectral changes of **1** in Figure 1, strong bleaching signals from the starting compound's CO-stretching band doublet at 1926 cm^{-1} and 1932 cm^{-1} are clearly observed at 8 ps time delay, indicating efficient photoexcitation and CO loss. A third bleach signal for the parent compound's highest frequency CO-stretch

occurs at 1990 cm^{-1} but is not examined in this study. A broad red-shifted absorption feature (relative to the doublet bleach feature) is observed around 1915 cm^{-1} that has been interpreted previously as arising from cooling of vibrationally hot species.[3b,c] At intermediate time delays up to 302 ps, two new absorption bands are observed at 1888 cm^{-1} and 1940 cm^{-1}. These two absorptions decrease in intensity as the time delay increases and eventually disappear together at 30 ns. As the two features at 1888 cm^{-1} and 1940 cm^{-1} decay in intensity, we note that the absorption intensity at 1880 cm^{-1} increases to generate a newly observed feature in the nanosecond time scale. Coincident with the growth of absorption intensity at 1880 cm^{-1}, another new absorption feature centered near 1934 cm^{-1} also emerges on top of the parent bleach feature. These results indicate that there are two new dicarbonyl species initially formed upon UV irradiation of **1** in *n*-heptane, and while one pair of CO bands disappears, the other pair grows suggesting they are kinetically coupled. We assign the blue shifted pair of CO-stretching bands at 1888 cm^{-1} and 1940 cm^{-1} to the Cr-solvate, and the red shifted pair of CO-stretching bands at 1880 cm^{-1} and 1934 cm^{-1} (identical to that observed in the difference FTIR at the bottom of Figure 1) to the Cr-S chelate. The overall chelation reaction mechanism is summarized in Scheme 2. These assignments are also consistent with previously obtained results from transient and steady-state IR studies of **4**, **5**, and **6** in *n*-heptane in which the metal-heptane solvate intermediate has CO-stretching bands blue-shifted relative to the CO–stretching bands of the metal-S chelate.[3b,c] Additional support for these spectral assignments are derived from previously reported observations that (arene)$Cr(CO)_2$-alkane complexes are observed with up to microsecond lifetimes.[12]

The difference TRIR spectral changes observed for **2** and **3** in heptane (see Figure 1) are similar to that of **1**. However, having additional sulfide groups on the pendant side chain appears to diminish the competing solvent coordination. Apparently solvent coordination is not completely excluded for **3** as was previously observed for the Mn analog.[2b] Examining the two overlapping absorption bands of **1** near 1880 cm^{-1} and 1888 cm^{-1} at 102 ps time delay, we note that the absorption intensity at 1880 cm^{-1} of the Cr-S chelate is approximately half the absorption intensity at 1888 cm^{-1} arising from the Cr-heptane solvate. Assuming the Cr-S chelate and the Cr-heptane solvate have similar IR absorption cross-sections, this result suggests that the initial Cr-S chelate/Cr-heptane solvate ratio is approximately 1:2. Applying the same analysis to the other Cr-S species, the initial Cr-S chelate/Cr-heptane solvate distribution is slightly larger than 1:2 upon the irradiation of **2** and ~ 2:1 upon the irradiation of **3**.

Previous conformational analyses of the manganese analogs **4**, **5**, and **6** showed that the most energetically favorable conformations of the manganese complexes position the side chain carbonyl group in the Cp ring plane (Cp = Cyclopentadienyl).[3b,c] As a result, the sulfide group in **4** is near the Mn metal center 50% of the time while all lowest energy conformations of **6** position a sulfide group near the Mn metal center all the time. Hence, the chelate:solvate population distribution immediately after photolysis of **4** and **5** is approximately 1:1, and there is no solvate observed after irradiation of **6** in *n*-heptane solution. If the initial product distribution depends on the side chain availability and the unsaturated metal center reacts with the first species it encounters,[3c] then the sulfide group(s) in **1** and **2** should be near the metal center at least ~33% of the time while a sulfide group for **3** would be near the metal center ~66% of the time to produce the above

observed initial product distribution. This argument would imply that conformational or other structural features position pendant sulfides better on the CpMn derivatives than benzene-Cr derivatives. For example, the potential well for rotation of the side chain carbonyl group relative to the arene ring may be deeper and therefore "narrower" for **4**-**6** compared to **1**-**3** forcing sulfide groups of **4**-**6** to generally spend more time near the metal. A more plausible explanation may be that the larger benzene ring holds the sulfide groups farther away from the metal center than the cyclopentadienyl ring. The lowest energy conformations determined by Density Functional Theory (DFT isolated molecule calculations using Gaussian 03 software) indicate that the nearest neighbor sulfur is 0.2 Å further away from the Cr compared to Mn. Finally DFT calculations reveal a higher charge on Mn (+2.1) versus Cr (+0.6) resulting in a greater attraction of the polar sulfide groups in the Mn complexes which may make chelation more probable.

Figure 2 shows transient difference spectra of **2** and **3** in THF solution recorded at pump-probe delay times ranging from picoseconds to milliseconds and FTIR difference spectra of **1**, **2**, **3**, and **7** (Scheme 2) before and after 30 seconds of UV irradiation with a xenon arc lamp (the FTIR spectral acquisition time was approximately 1 min). Since **7** has no chelatable side chain, we conclude that irradiation of **7** in THF yields the Cr-THF adduct, **8**, having characteristic IR bands at 1842 cm^{-1} and 1906 cm^{-1}. These same absorption bands, also observed in the difference TRIR experiments, are therefore assigned to the Cr-THF solvate. Apparently, the chelation dynamics of **1**, **2**, and **3** in THF are similar to that observed in *n*-heptane with the exception that the dominant chelation pathway in THF is via the Cr-THF solvate. It is more difficult to obtain good signals in THF because unlike *n*-heptane; THF strongly absorbs in the IR region of the

photoproducts. The picosecond timescale signals are also weaker due to much lower available UV pump pulse power. We did not study the chelation of **1** on the picosecond timescale because the results obtained from nanosecond experiments and studies in *n*-heptane suggested that there would be no significant difference in the chelation dynamics between **1** and **2**. In any event, broad absorptions (*ca*. 30 cm^{-1} full-width at half-maximum (FWHM)) near 1842 cm^{-1} from **1** and **2** and 1858 cm^{-1} from **3** are observed, particularly in the nanosecond regime which remained unchanged up to microsecond time delays (not shown). The fact that the full-width at half maximum of these features are *ca*. 1.5 times broader than all other bands observed in the difference FTIR spectra, and that their base widths extend beyond the overlaying absorptions of the chelate and the solvate as observed in the difference FTIR spectra, implies they are composed of more than one CO-stretching bands. The two additional bands near 1906 cm^{-1} and 1918 cm^{-1} are largely obscured by the parent species bleach band at 1906 cm^{-1}. The combined results from the TRIR and steady-state FTIR experiments indicate that the solvate Cr-THF species eventually converts to the Cr-S chelate on greater than 5 ms timescales. Using the difference TRIR spectra at 10 ns where the best signal-to-noise ratio for all three complexes was obtained, we note that the absorption intensity at 1858 cm^{-1} is approximately 0.33 the absorption intensity at 1842 cm^{-1} from the irradiation of **1** and **2**, but both of the intensities are the same from irradiation of **3**. Our TRIR spectrometer can monitor spectral changes up to 5 ms, however the FTIR difference spectra show that the final products of **1**, **2**, and **3** are not the Cr-THF solvates but the Cr-S chelates. These results indicate that (1) the ultrafast coordination of solvent is more favorable for the stronger coordinating solvent and therefore chelation in THF occurs mainly via the Cr-

solvate and (2) the stronger the Cr-solvent bond,[13] the longer time it takes for the Cr-solvate to convert to the Cr-S chelate.

Figure 3 shows transient difference spectra for **1**, **2**, and **3** in acetonitrile recorded at pump-probe delay times ranging from -4 ps to 80 ps. Unlike the results obtained from irradiation of **1**, **2**, and **3** in *n*-heptane and THF, the spectral changes observed for all three complexes in acetonitrile are nearly identical. A bleach band from the starting compound is clearly observed at 1905 cm^{-1} (the second high frequency bleach band occurs at 1977 cm^{-1} and was not examined). For delay times greater than 23 ps, a broad absorption band (ca. 20 cm^{-1} full-width at half-maximum (FWHM)) appears at 1846 cm^{-1}. When the transient spectra are overlapped (see Figure 4), we observe isosbestic points near 1895 cm^{-1} and 1860 cm^{-1} which indicates a clean conversion from the parent tricarbonyl molecule to a photoproduct. The transient spectral changes after 27 ps are nearly identical to those obtained from the steady-state experiments (bottom of Figure 3). The acetophenone chromium tricarbonyl complex **7** has similar ground state CO-stretch absorption bands (appear as bleaches in the difference FTIR spectra) as those of **1**, **2**, and **3**, and the FTIR difference spectrum obtained by steady-state irradiation of **7** producing **9** (Scheme 3) in acetonitrile results in nearly identical TRIR difference spectra of **1**, **2**, and **3** in acetonitrile. Despite many attempts to prepare Cr-S chelates in acetonitrile, they could not be isolated or observed, whereas stable isolated chromium acetonitrile complexes are known.[14] These results suggest that the bond energies of the Cr-S chelate and the Cr-solvate are most likely in the order Cr-heptane < Cr-THF < Cr-S (chelate) ≤ Cr-acetonitrile, and are consistent with relative bond energies reported for other metal carbonyl complexes.[3c,15] If the initial product distribution upon irradiation of **1**, **2**, and **3**

is determined not only by the accessibility of the sulfide group but also by the coordination power (as was observed from the TRIR experiments in *n*-heptane and THF), then the transient TRIR experimental results suggest that irradiation of **1**, **2**, and **3** in acetonitrile yields the Cr-$NCCH_3$ solvate, with no evidence for sulfur chelation.

Conclusions

The results from this investigation indicate that the reaction rates and chelation pathways of the chromium series (1-3) complexes depend on the steric accessibility of the chelatable side group. These substitution reactions are also influenced by the structure of the side chain, type of the chelable ligand, the metal center, and coordination power of the solvent. We found that there is competition between immediate chelation and solvent coordination following CO dissociation of **1**, **2**, or **3** in *n*-heptane and THF solutions to form two initial products: Cr-S chelate and Cr-Sol (Sol = *n*-heptane or THF) solvate which is similar pattern observed for the analogous manganese compounds (**4**-**6**). Adding sulfide groups to the chelatable side chain diminishes the solvation pathway, but there is no evidence for solvent exclusion as previously observed for the manganese compound (**6**). More reactive solvents which form stronger metal-solvent bonds favor the solvation process to the extent that Cr-S chelation does not occur in acetonitrile. Depending on the solvent, the conversion time from the solvate to the Cr-S chelate depends on the metal-solvent bond energy where the weaker associating solvent is most rapidly replaced. This study highlights how subtle structural changes may be used to tailor picosecond processes for the design of ultrafast molecular switches. More

extensive studies are under way where the multiplicity of the electronic state will be considered.

Acknowledgments:

This work was partly supported by the National Science Foundation under Grant No. CHE-0227475 (T.J.B.) and internal NIST Scientific, Technical and Research Services funding (C.B.D., T.T.T. and E.J.H.). We also thank Dr. Okan Essenturk (U. Maryland NIST Guest Researcher) for his valuable discussions and help with molecular structure DFT calculations.

References and notes

[1] (a) For leading references on photochromic materials in photonic devices see Irie, M. Ed. *Chem. Rev*. **2000**, *100*, 1683. (b) For a recent review on the use of photochromic materials for optical switches see Raymo, F. A.; Tomasulo, M. *Chem. Eur. J.* **2006**, *12*, 3186.

[2] To, T. T.; Barnes, C. E.; Burkey, T. J. *Organometallics* **2004**, *23*, 2708.

[3] (a) To, T. T.; Burkey, T. J.; Heilweil, E. J. *J. Phys. Chem. A* **2006**, *110*, 10669. (b) Yeston, J. S.; To, T. T.; Burkey, T. J.; Heilweil, E. J. *J. Phys. Chem. B* **2004**, *108*, 4582. (c) Jiao,T.; Pang, Z.; Burkey, T. J.; Johnston, R. F.; Heimer, T. A.; Kleiman, V. D.; Heilweil, E. J. *J. Am. Chem. Soc.* **1999**, *121*, 4618.

[4] (a) Wiland, S.; van Eldik, R. *J. Phys. Chem.* **1990**, *94*, 5865. (b) Burdett, J. K.; Grzybowski, J. M.; Perutz, R. N.; Poliakoff, M.; Turner, J. J.; Turner, R. F. *Inorg. Chem.* **1978**, *17*, 147.

[5] (a) Lian, T.; Bromberg, S. E.; Asplund, M. C.; Yang, H.; Harris, C. B. *J. Phys. Chem.* **1996**, *100*, 11994. (b) Kim, S. K.; Pedersen, S.; Zewail, A. H. *Chem. Phys. Lett.* **1995**, *233*, 500. (c) Schwartz, B. J.; King, J. C.; Zhang, J. Z.; Harris, C. B. *Chem. Phys. Lett.* **1993**, *203*, 503.

[6] Barbero, M.; Cdamuro, S.; Degani, I.; Dughera, S.; Fochi, R. *J. Org. Chem.* **1995**, *60*, 6017.

[7] H^1-NMR (270 MHz, $CDCl_3$, 298 K): δ 2.15 (s, 3H, SCH_3), 3.84 (s, 2H, CH_2), 5.27 (m, 2H, C_6H_5), 5.65 (m, 1H, C_6H_5), 6.12 (m, 2H, C_6H_5).

[8] H^1-NMR (270 MHz, $CDCl_3$, 298 K): δ 2.11 (s, 6H, 2(SCH_3)), 4.88 (m, 1H, CH), 5.25 (m, 2H, C_6H_5), 5.66 (m, 1H, C_6H_5), 6.16 (m, 2H, C_6H_5).

[9] H^1-NMR (270 MHz, $CDCl_3$, 298 K): δ 2.06 (s, 9H, 3(-SCH_3)), 5.18 (m, 2H, C_6H_5), 5.69 (m, 1H, C_6H_5), 6.80 (m, 2H, C_6H_5).

[10] Certain commercial equipment, instruments, or materials are identified in this paper in order to adequately specify the experimental procedure. In no case does such identification imply recommendation or endorsement by NIST, nor does it imply that the materials or equipment identified are necessarily the best available for the purpose.

[11] Mahaffy, C.; Pauson, P. L. *Inorg. Synth.* **1990**, *28*, 136.

[12] (a) Creavens, B. S.; George, M. W.; Ginsburg, A. G.; Hughes, C.; Kelly, J. M.; Long, C.; McGrath, K. M.; Pryce, M. T. *Organometallics* **1993**, *12*, 3127. (b) Walsh, E.

F.; George, M. W.; Goff, S.; Nikiforov, S. M.; Popov, V. K.; Sun, X.-Z.; Poliakoff, M. *J. Phys. Chem.* **1996**, *100*, 19425-19429.

[13] Our previous studies showed that the metal-ligand bond strength with other metal complexes is in the order of M-alkane << M-O < M-S (see reference 3c).

[14] Ross, B. L.; Grasselli, J. G.; Ritchey, W. M.; Kaesz, H. D. Inorg. Chem. **1963**, *5*, 1023.

[15] Farrell, G. J.; Burkey, T. J. *J. Photochem. Photobiol. A: Chemistry* **2000**, *137*, 135.

Chart 1

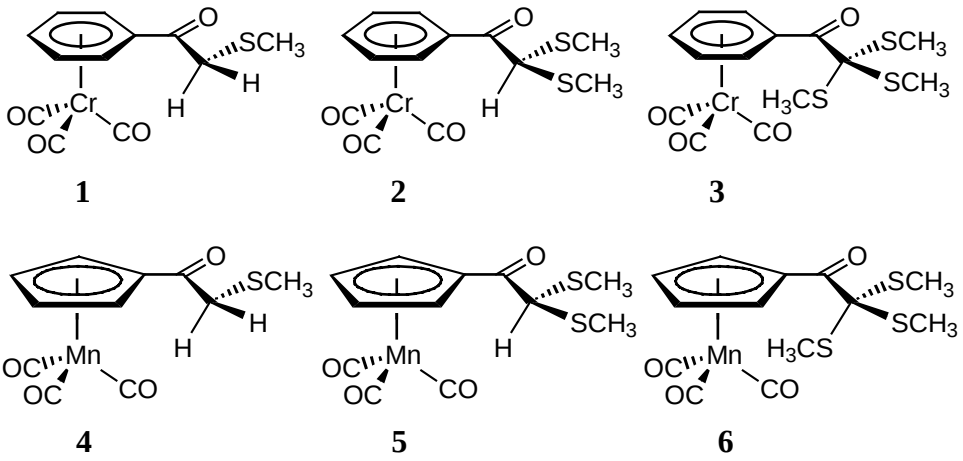

Scheme 1

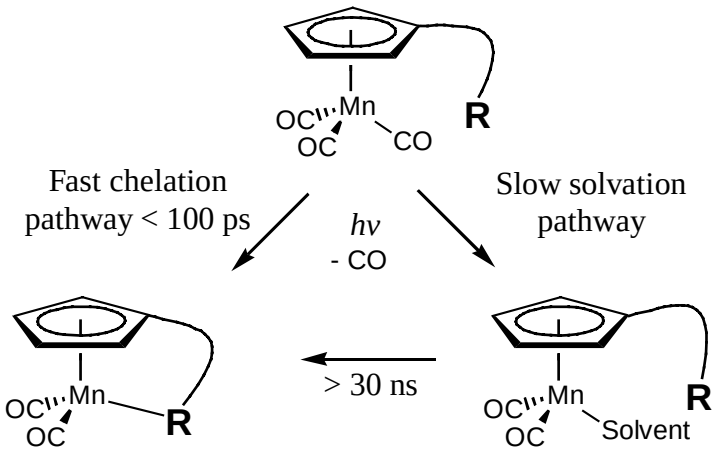

Scheme 2

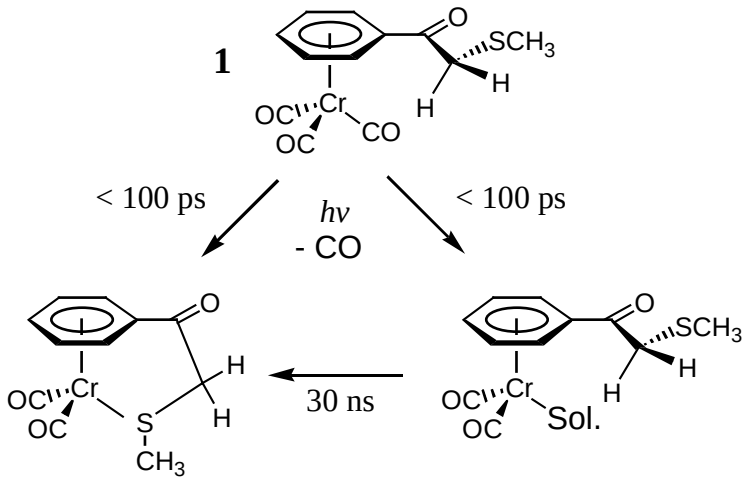
1
O
SCH3
H
OC
Cr
CO
OC
< 100 ps
hν
- CO
< 100 ps
O
H
OC
Cr
H
OC
S
CH3
30 ns
O
SCH3
H
H
OC
Cr
OC
Sol.

Scheme 3

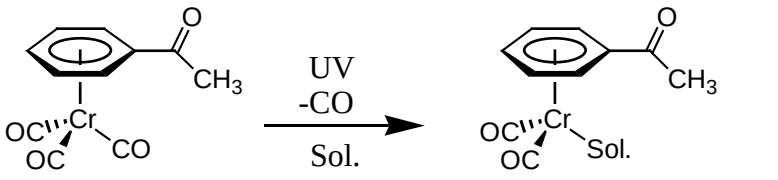

7

8 Sol. = THF

9 Sol. = $NCCH_3$

Figure Captions

Figure 1. Transient TRIR difference spectra acquired after UV irradiation of **1**, **2**, and **3** in *n*-heptane at 298 K. Presented within each labeled time delay the thickest, medium, and thinnest spectral lines correspond to spectral changes of **1**, **2**, and **3**, respectively. At each time delay, the spectra are offset vertically by 0.01 OD units for clarity. At the bottom are the difference FTIR spectra of **1**, **2**, and **3** (amplitude divided by a factor of 3) in *n*-heptane acquired before and after irradiation with a xenon arc lamp.

Figure 2. Transient TRIR difference spectra acquired after UV irradiation of **1**, **2,** and **3** in THF at 298 K. **1** was not investigated for picosecond delay times because it showed similar dynamics to **2** in n-heptane (see Fig. 1). At each time delay, the spectra are offset vertically by 0.01 OD units for clarity. At the bottom are difference FTIR spectra of **1**, **2**, **3**, and **7** (amplitude divided by a factor of 2) in THF acquired before and after irradiation with a xenon arc lamp.

Figure 3. TRIR difference spectra acquired after UV irradiation of **1**, **2**, and **3** in acetonitrile at 298 K. The spectra are offset vertically by 0.01 OD units for clarity. At the bottom are difference FTIR spectra of **1**, **2**, **3**, and **7** (amplitude divided by a factor of 2) in acetonitrile acquired before and after irradiation with a xenon arc lamp.

Figure 4. Overlapped transient TRIR difference spectra from Figure 3 of **1**, **2**, and **3** in acetonitrile at 298 K highlighting two isosbestic points at 1895 cm^{-1} and 1860 cm^{-1}. The lightest and darkest spectra were obtained at 13 ps and 107 ps time delays, respectively. The two intermediate time-delayed spectra were obtained at 40 ps and 90 ps where the 40 ps spectrum has the second strongest bleach intensity near 1905 cm^{-1}.

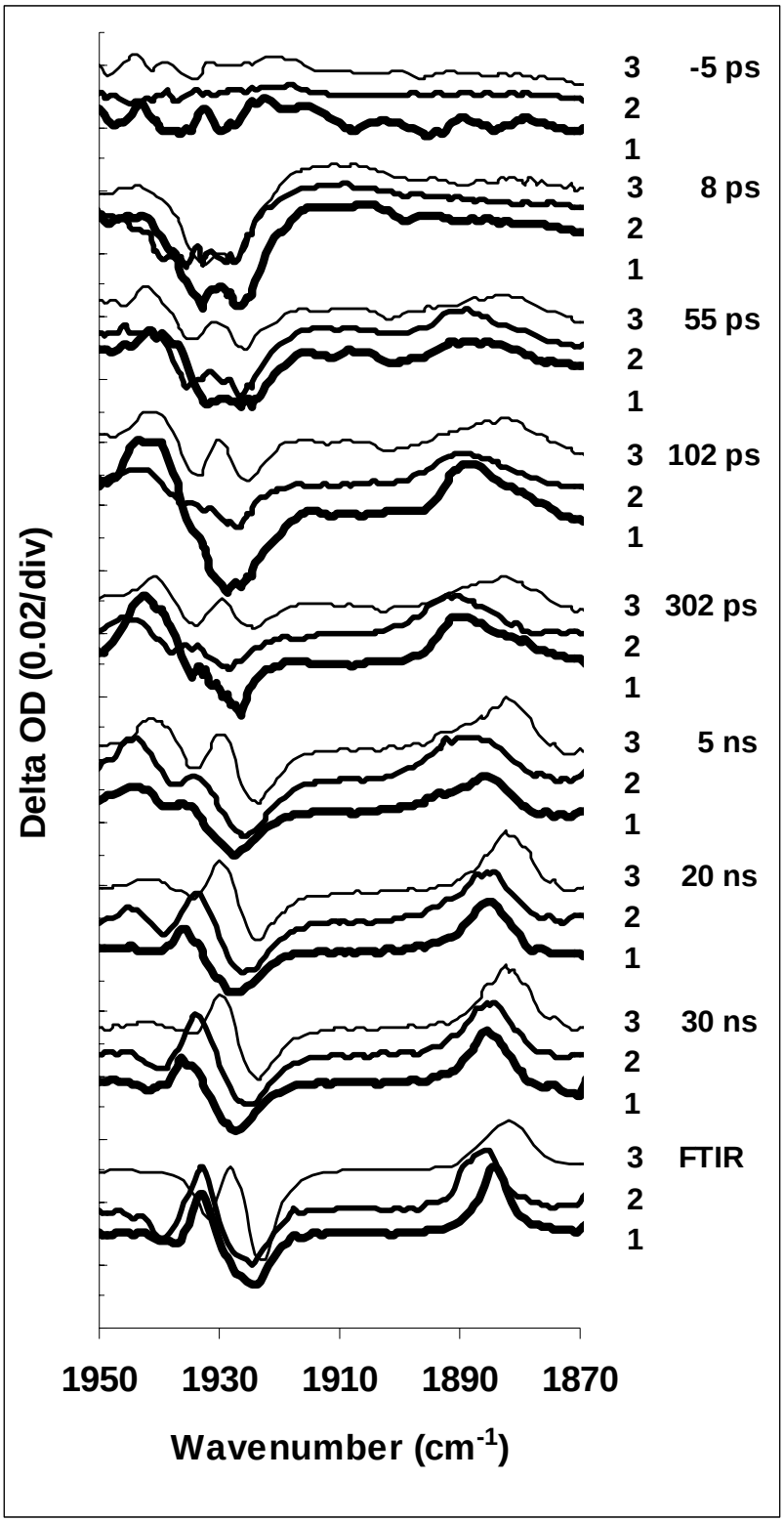

Figure 1 – To et al, J. Phys. Chem.

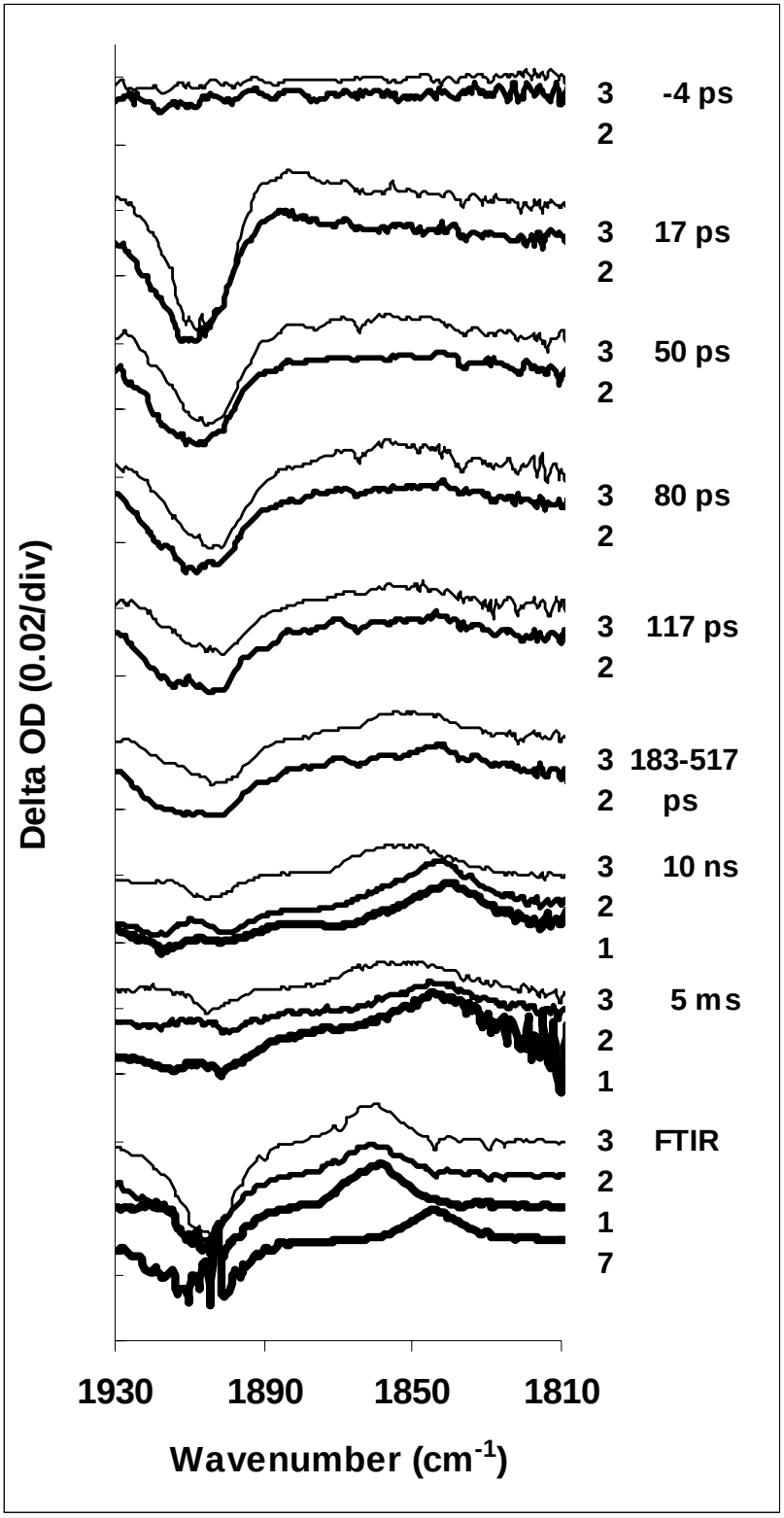

Figure 2 – To et al, J. Phys. Chem.

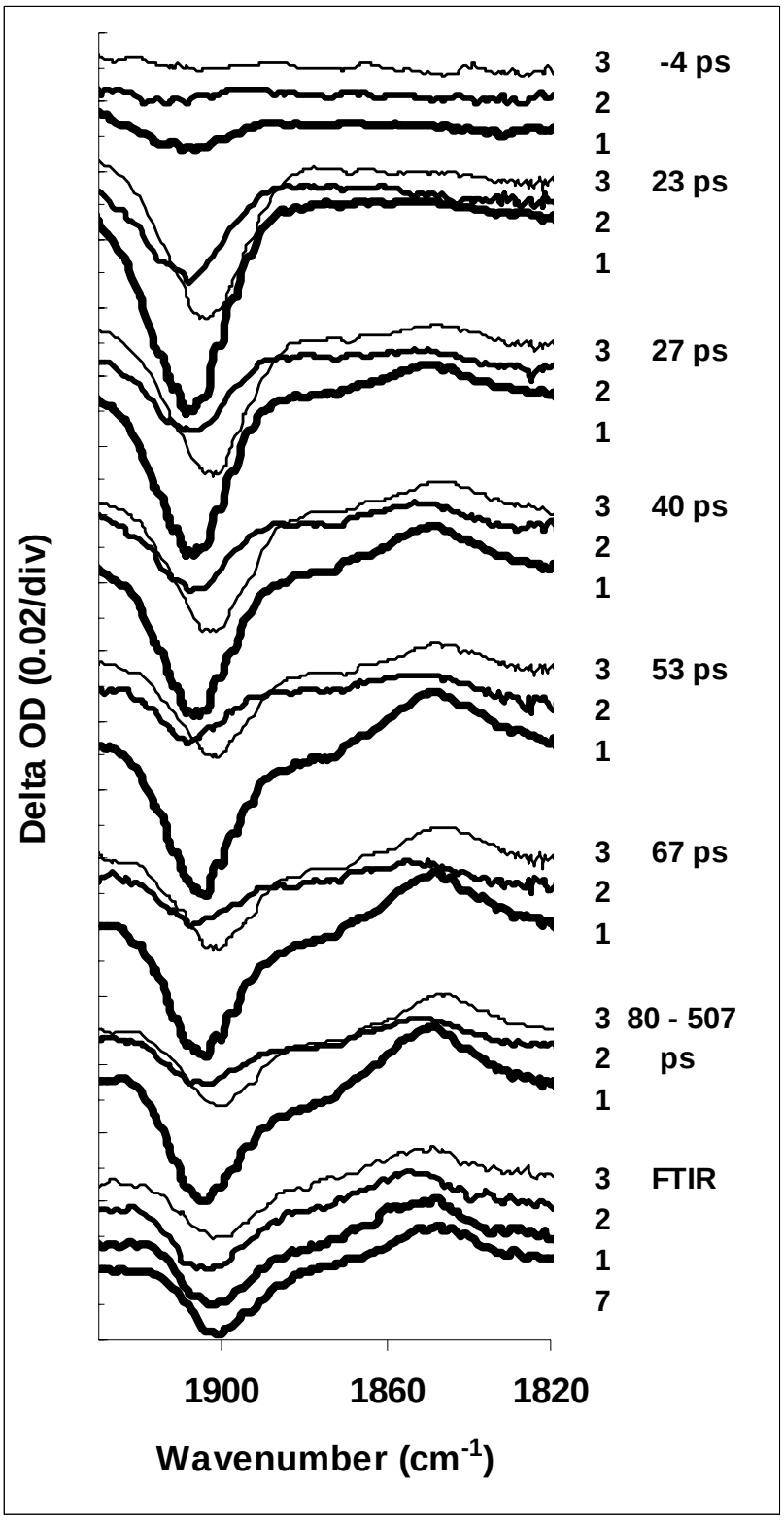

Figure 3 – To et al, J. Phys. Chem.

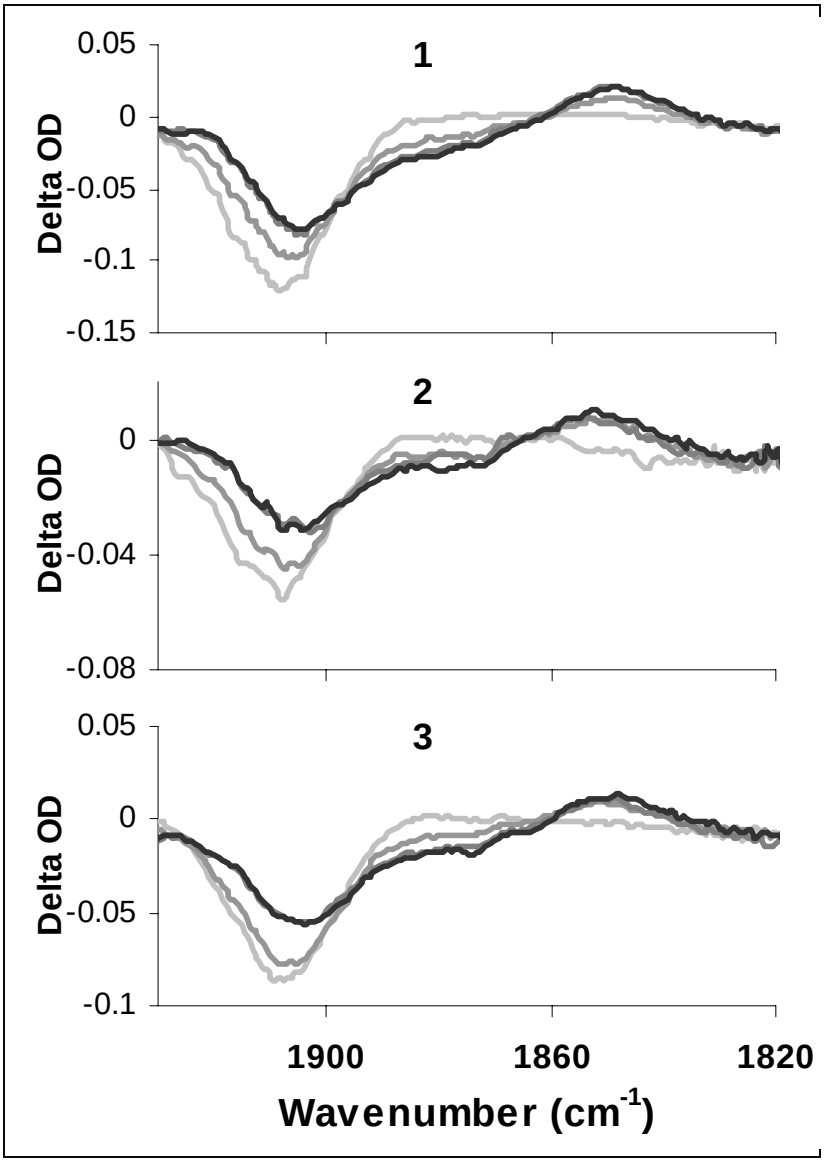

Figure 4 – To et al, J. Phys. Chem.